Egypt. J. Bot. **Vol. 58,** No. 3, pp. 563 - 579 (2018)

Bioremediation and Extracellular Synthesis of Copper Nanoparticles from Wastewater using *Yarrowia lipolytica* AUMC 9256

Manal Tawfeek El-Sayed
Botany Department, Faculty of Science, Zagazig University, Zagazig, Egypt.

THIS THE FIRST study describing the rapid extracellular synthesis of copper nanoparticles during the bioremediation of copper by living, autoclaved and dried biomass of *Yarrowia lipolytica* AUMC 9256. The time course growth in the presence of different concentrations of Cu(II) was studied. The minimum inhibitory concentration value of *Y.lipolytica* AUMC 9256 for Cu(II) was 1900mg/L. The cellular localization of bioaccumulated copper ions was assessed. Maximum uptake capacities were accomplished at pH 6.0, initial metal ion concentration 450mg/L, biomass dosage 1g/L and contact time 180min for live cells, 90min for autoclaved and 30min for dried biomass. Copper nanoparticles were characterized by UV-Visible spectrophotometer and transmission electron microscopy. They were all spherical in shape with an average size of 32.85nm (live), 22.34nm (autoclaved) and 15.62nm (dried). The occurrence of extracellular complexation, precipitation, adsorption onto cell wall and sequestration of needle-, rod-shaped precipitates within central large vacuole during Cu(II) uptake by live biomass were found out by transmission electron microscopy. Fourier Transform Infrared spectroscopy confirmed that mannans, phosphorus, P=S stretching, C-S stretching, M-O and ring deformation were more included in Cu(II) uptake by dried biomass. Energy dispersive X-ray microanalysis confirmed the presence of high-intensity characteristic peaks of Cu(II) and a sharp reduction of atomic % of phosphorus and potassium on the cell wall. X-ray powder diffraction patterns of Cu(II)-loaded biomass confirmed their crystalline nature. The removal of copper from ceramic industry wastewater was carried out by dried biomass effectively.

Keywords: *Yarrowia lipolytica*, Biosorption, Copper, Mechanism, Nanoparticles.

Introduction

Heavy metal pollution has become one of the most serious problems in developing countries as a result of industrialization, which produces large quantities of wastewaters containing heavy metals in natural environments and consequently in food chains (Adams et al., 2015). Unlike organic contaminants, heavy metals are non-biodegradable and some of them could be transformed from low toxic species into more toxic forms and damage normal physiological activities (Anju, 2017).

Although copper (Cu(II)) is an essential microelement for all living organisms because it is a key constituent of the respiratory enzyme complex cytochrome oxidase, an accumulation of high concentrations of it can be toxic to a wide variety of organisms, especially microbial populations (Ali et al., 2013). High concentrations of Cu(II) catalyzes the synthesis of reactive oxygen species ($O^{\bullet-}_2$, $^1O_2$, $OH^{\bullet}$, H_2O_2, etc.) leading to severe damage of cytoplasmic constituents (Buss, 2012).

Cu(II) was chosen for this study with regard to its wide use in industry and potential pollution impact. In the copper-cleaning, copper plating and metal-processing industries, Cu(II) concentrations approach 100–120mg/L; this value is very high in relation to water quality standards (Sağ et al., 1995) and should be reduced to a value of 1.3mg L^{-1} according to WHO (2004).

During the last few decades, many research efforts have been involved in heavy metal binding to non-living and living biomass from wastewater streams (Karbassi et al., 2016). Microorganisms can sustain themselves in a toxic metallic environment, accumulate and transform toxic metals to nontoxic metals in various ways like bioaccumulation, biosorption, and biotransformation (Vijayaraghavan & Balasubramanian, 2015). Siddiqi & Husen (2016) mentioned that biogenic synthesis of metal nanoparticles (NPs) involves bioreduction of metal salts to elemental metal and biosorption where metal ions in the aqueous medium are

Corresponding author email: tawfeek.manal1@gmail.com Tel: 01117132152
Edited by: Prof. Dr. Salama A. Ouf, Faculty of Science, Cairo University, Cairo, Egypt
DOI: 10.21608/ejbo.2018.3047.1157

bonded to the surface of the cell wall of the organisms.

In fact, *Yarrowia lipolytica* has been used for bioremediation applications due to its cell wall characteristics and surfactant production (Coelho et al., 2010). Resting and actively growing cells of two strains of *Y. lipolytica* were used for mercury bioremoval (Oyetibo et al., 2016). Biosorption of Cu(II) by live and dead cells of *Y. lipolytica* was studied by Wierzba (2014). The inactivation of microbial cells (e.g. wet or dry thermal treatment), modifies the surface characteristics/ groups by masking or removing the groups or exposing more chemical binding sites (Dhankhar & Hooda, 2011). However, the status of biomass, types of biomaterials, properties of metal solution chemistry and biosorption conditions will all affect the mechanism of metal uptake (Akinkunmi et al., 2016).

The primary goal of this study was to: (i) Determine biosorption potential of living, autoclaved and dried cells of *Y. lipolytica* AUMC 9256 for Cu(II) ions under different parameters, (ii) Study the growth pattern of *Y. lipolytica* AUMC 9256, removal efficiency, the release of potassium and calcium and localization of accumulated Cu(II), (iii) Characterize the mycosynthesized copper nanoparticles (Cu NPs) and (vi) Determine the possible mechanisms of Cu(II) uptake by *Y. lipolytica* AUMC 9256.

Materials and Methods

The microorganism, maintenance and preparation of Y. lipolytica AUMC 9256 biomass

Y. lipolytica AUMC 9256 obtained from Assuit University Mycological Centre was maintained on YPD agar slants containing (g/L): Yeast extract, 10; glucose, 20; peptone, 20 and agar, 15. Slants were incubated at 30^0C for 48h, subsequently stored at 4^0C and subcultured at regular intervals. In order to determine the biosorption potential, the strain was cultured in 500ml Erlenmeyer flasks containing 100ml YPD broth medium on a rotary incubator shaker at 120rpm. Yeast cells were harvested by centrifugation at 6000rpm for 10min at 4^0C. Thereafter, live, autoclaved and dried biomass was prepared according to Huang et al. (2013). The dry weight of the biomass was determined for each set.

Preparation of metal solution.

The solution of Cu(II) at a concentration of 2000mg/L was prepared by dissolving appropriate amounts of $CuSO_4.4H_2O$ in deionized water. Other metal ion concentrations were achieved by subsequent diluting the solutions with deionized water. All chemicals were of analytical grades.

Copper tolerance test and determination of minimum inhibitory concentration (MIC)

One hundred µl of yeast suspension (1×10^6CFU/ml) was inoculated onto YPD plates supplemented with the sterilized $CuSO_4.4H_2O$ solution to get the final concentration ranged from 0 to 2000mg/L concentration of Cu(II). After 5 days of incubation, the metal MIC value was evaluated in terms of the first concentration at which no growth of *Y. lipolytica* was observed.

Effect of different concentrations of Cu(II) on the growth of Yarrowia lipolytica AUMC 9256

Aliquots were harvested from the exponential growth phase and were inoculated in 250 Erlenmeyer flasks containing 50ml yeast nitrogen base (YNB)-glucose broth medium (to avoid possible interaction of metal ions with complex components of the media) supplemented with copper sulphate solution in varying concentrations ranging from 0 to 800mg/L (Paš et al., 2004). YNB-glucose contained (in g/L): Yeast nitrogen base without amino acids, 6.7 and glucose, 20. Ambient pH was adjusted to 5.5 with 0.1N NaOH and 0.1N HCl. Media inoculated with the yeast strain only (without Cu(II)) and media amended with different concentrations of Cu(II) (without yeast strain) were included as controls. Samples (2ml) were taken every 8h and monitored for turbidity via optical density at 600nm. All the experiments were run in triplicates and the mean values were estimated.

To determine the removal efficiency (R_e%), *Y. lipolytica* AUMC 9256 growth suspension (grown in the YNB-glucose amended with different concentrations of Cu(II), as described earlier) was centrifuged and the supernatant was analyzed for the residual Cu(II) ions by using an atomic absorption spectrophotometer (Model Unicam 969, Centric Laboratory of Agriculture Faculty, Zagazig University). R_e% was calculated according to the following equation:

$$R_e\ (\%) = C_i - C_e / C_i\ 100\times$$ (Shanab et al. 2012).

where C_i and C_e are the initial and residual Cu(II) concentrations (mg/L), respectively.

Elemental K(I) and Ca(II) analysis

Analysis of Ca(II) and K(I) contents of the supernatant of metal-free and Cu(II)- loaded pellets sorption solutions was done using atomic absorption spectrophotometer.

Cellular distribution of Cu(II)

The distribution of bioaccumulated Cu(II) was determined according to Huang et al. (2013).

Batch biosorption experiments

The effect of pH (2-6), initial metal ion concentration (50-500mg/L), biosorbent mass (1-5g/L) and contact time (5min-24h) on the removal of Cu(II) was evaluated. The batch biosorption experiments were performed in 500ml Erlenmeyer flasks with 100ml of metal solution. Different concentrations of Cu(II) were prepared by proper dilution of Cu(II) stock solution. The initial pH of metal solutions was adjusted with 1N NaOH or 0.1N HCl. The required biomass dose (with respect to cell dry weight) was thereafter added and the content of the flask was shaken (120rpm) at 30^0C. Then, Cu(II) solution was separated from the biomass by filtration. The residual Cu(II) ion concentration in the filtrate was measured by using an atomic absorption spectrophotometer. Sorption contact experiments were carried out in triplicate and the mean values were considered. For all graphical representations, standard error bars were plotted. The biosorption capacity (q_{eq}) was calculated from the following equations:

$$qeq = Ci - Ceq/m \times V$$

where q_{eq} is metal uptake capacity (mg of metal/g of sorbent), C_i and C_{eq} are the initial and equilibrium Cu (II) concentration (mg/L), respectively, m is the sorbent mass (g dry cell/L) and V is the volume of aqueous phase.

Characterization of Cu NPs synthesized by Y. lipolytica AUMC 9256

Y. lipolytica AUMC 9256 biomass were suspended separately in 1000ml of 450mg/L concentration of Cu (II) under the optimum conditions. After centrifugation, the supernatants were then passed through 0.22µm filter to make them cell-free (CFS). Cu NPs were characterized by UV-Visible spectroscopy measurements (T80 UV–Vis spectrophotometer, Germany). The size and shape of Cu NPs were determined by transmission electron microscopy (TEM) investigations (a JEOL TEM -1400 electron microscope and optronics AMT CCD camera with 1632 pixel format as side mount configuration). Samples for TEM were prepared by placing a drop of Cu NPs solution onto a carbon-coated copper grid and allowing the drop to dry at room temperature.

Mechanism of Cu(II) uptake

TEM investigation

Part of the obtained pellets before and after Cu(II) exposure was subjected to TEM investigation to ascertain the cellular localization of accumulated Cu NPs and understand the uptake mechanism. Transmission and photographing were done using a JEOL-1010 electron microscope (Regional Center of Mycology and Biotechnology, Cairo, Egypt). To distinguish the functional groups involved in the uptake, FTIR of metal-free, live, autoclaved and dried Cu(II)-loaded biomass were recorded over the region 400-4000cm^{-1} with Perkin-Elmer FTIR 1650 spectrophotometer. The samples were examined in KBr discs. To study the elemental analysis of the biomass, the biosorbents before and after Cu NPs synthesis were analyzed by X-ray microanalyzer (EDX) (Model Oxford 6587 INCA x-sight) attached to JEOL JSM-5500 LV scanning electron microscope. XRD pattern of powder samples of Cu(II)-free (control) and Cu(II)-sorbed live, autoclaved and dried biomass was recorded in a Broker D8 Advanced target Cukα powder diffractometer (λ=1.5418Å) over the range of 0-80(2θ).

Application of dried Y. lipolytica AUMC 9256 biosorbent to environmental samples

The applicability of dried *Y. lipolytica* AUMC 9256 biosorbent in the adsorptive removal and treatment of water from Cu(II) was examined by a multistage microcolumn technique. Ceramic wastewater was collected from a ceramic factory in Industrial area of Tenth of Ramadan, Sharkia, Egypt. Temperature and pH values were measured. Water samples were filtered through a 0.45µm membrane filter and then analyzed to identify the concentrations of Cu(II). Adsorptive removal of Cu(II) from water sample was performed by passing 1L solution through a glass microcolumn (length = 10cm and internal diameter = 0.5cm) packed with 1g of dried *Y.*

lipolytica biosorbent under constant flow rate (10ml/ min) (Mahmoud et al., 2017).

Results

Cu(II) tolerance by Y. lipolytica AUMC 9256

Determination of MIC

The yeast strain was found to be tolerant to 1900mg Cu(II)/L. Colonies developed in the presence of >200mg Cu(II)/L became much darker than control ones.

Growth pattern of Y. lipolytica AUMC 9256 in the metal-containing media

The growth of the yeast strain was initially increased at 100mg Cu(II)/L of in respect to control followed by a gradual decrease with further increase in Cu(II) concentration (Fig. 1). A complete inhibition was observed at 800mg Cu(II)/L.

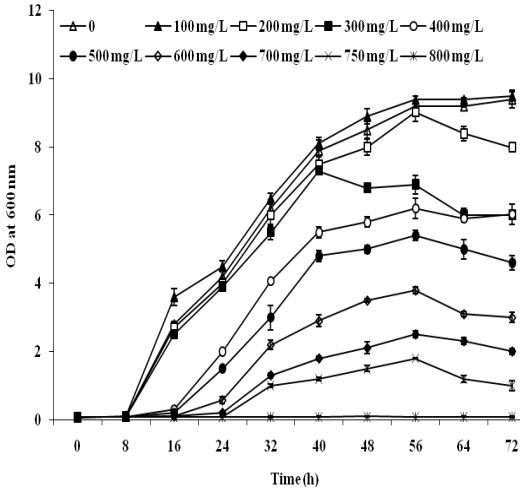

Fig. 1. Growth pattern of *Y. lipolytica* AUMC 9256 in the absence and presence of different initial concentrations of Cu (II) at 30°C, 150rpm and initial pH 5.5.

Figure 2 indicated that at low Cu(II) concentration (100mg/L), the value of R_e% was found to be 89.8. A gradual increase in Cu(II) concentration was accompanied by a gradual decline in R_e% and reached its minimum value (15.4%) at 750mg Cu(II)/L.

Release of (K) and Ca(II)

Compared to metal-free biomass solution, the Cu(II)- biomass sorption solution showed the presence of substantial amounts of K(I) and Ca(II) (Table 1).

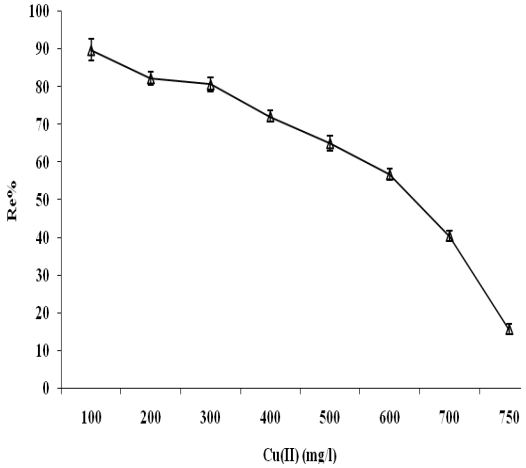

Fig. 2. Removal efficiency (Re%) of Y. lipolytica AUMC 9256 at different initial concentrations of Cu(ll) in liquid media.

TABLE 1. Release of K(I) and Ca(II) ions as a result of Cu(II) uptake by *Y. lipolytica* AUMC 9256.

Conc. of Cu(II) (mg/L)	Conc. of Ca(II) (mg/L)	Conc. of K(I) mg/L
0	0.045	0.069
100	0.061	0.105
200	0.09	0.18
300	0.10	0.25
400	0.15	0.34
500	0.27	0.61
600	0.36	0.78
700	0.51	0.8
750	0.68	0.91

Cellular distribution of bioaccumulated Cu(II)

As illustrated in Fig. 3, with an increase in Cu(II) concentrations from 100mg/L to 750mg/L, EDTA washable fraction (tightly cell surface bounded Cu(II)) was decreased from 35.8 to 12.1% while EDTA non washable fraction (intracellular bounded Cu(II)) was increased from 60.1 to 85.2 %.

Biosorption results

Effect of pH

Figure 4 showed that the values of Cu(II) biosorption capacities of the tested biomass were close to each other at low pH (2.0). With an increase in pH, the binding of ions was increased and the highest Cu(II) biosorption capacity was achieved at pH 6. Subsequent biosorption experiments were performed at pH 6. The Cu(II) biosorption capacity of dried cells was higher than that of autoclaved and live ones.

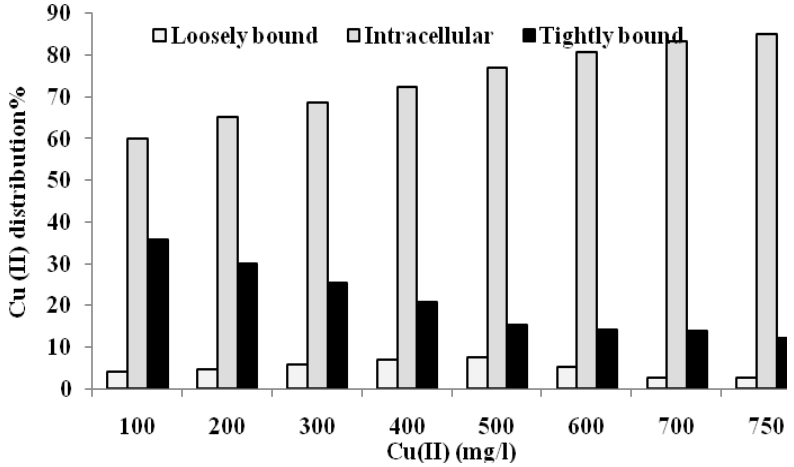

Fig. 3. Cu(ll) distribution percentage in different cellular compartments of *Y. lipolytica* AUMC 9256.

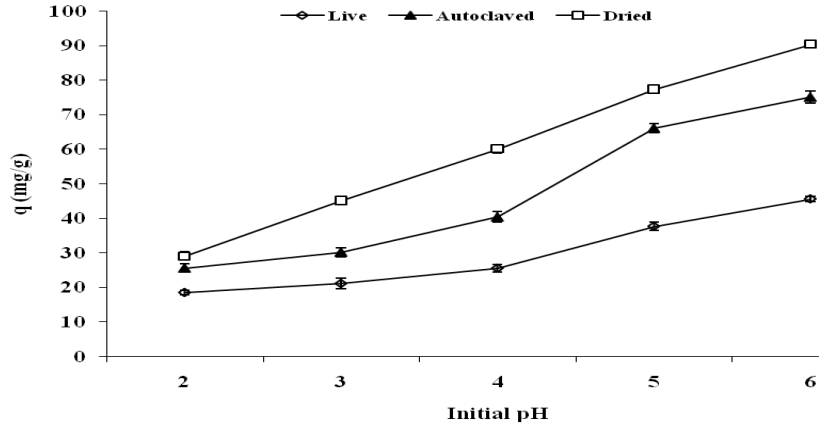

Fig. 4. Effect of initial pH on Cu(ll) uptake capacity of live, autoclaved and dried biomass of *Y. lipolytica* AUMC 9256. Biosorption conditions: Initial metal ion concentration(Ci) =450mg/L, biosorbent dose (m) = 1g/L, contact time (t) =180min (live biomass), 90min (autoclaved biomass) and 30min (dried biomass).

Effect of initial metal ion concentration of Cu(II)

Figure 5 showed that the uptake capacities of *Y. lipolytica* AUMC 9256 was increased from 10.2 to 46.5mg/g **(**live biomass), 14.1 to 77.8mg/g (autoclaved biomass) and 15.4 to 85.3mg/g (dried biomass) with an increase in Cu(II) concentration from 50 to 450mg Cu(II)/L. At 500mg/L concentration of Cu(II), the sites available for binding become fewer as compared with the molecules of the solute present. Subsequent biosorption experiments were carried out at 450mg/L of Cu(II) as initial metal ion concentration.

Effect of biosorbent dose of Y. lipolytica AUMC 9256

At minimum biosorbent dosage (1g/L), the maximum biosorption capacity was attained, which was 50.1mg/g for live biomass, 90.3mg/g for autoclaved biomass and 106.2mg/g for dried biomass (Fig. 6). With the increase of biomass dosage to 5g/L, the uptake of Cu(II) unanimously decreased to 7.1mg/g, 17.8 and 25.1mg/g for a living, autoclaved and dried biomass, respectively.

Effect of contact time

The effect of contact time on biosorption of Cu(II) by *Y. lipolytica* AUMC 9256 biomass was studied under optimal conditions (Fig. 7). Biosorption has occurred rapidly within 5-90min for live biomass, 5-50min for autoclaved biomass and 5-30min for dried biomass. The biosorption processes became slower from 90 to 180min for live biomass, 50 to 90min for autoclaved biomass and 90 to 180min for dried biomass. Equilibrium was reached within 3h (live biomass), 1.5h (autoclaved biomass) and 30min (dried biomass).

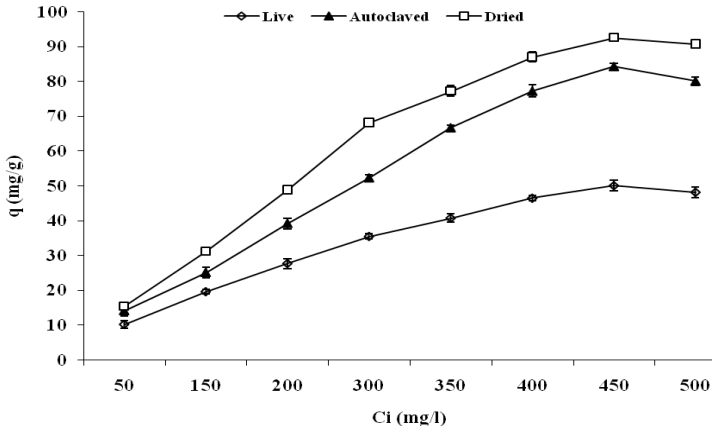

Fig. 5. Effect of initial metal ion concentration (Ci) of Cu(ll) on uptake capacity of live, autoclaved and dried biomass of *Y. lipolytica* AUMC 9256. Biosorption conditions: Initial pH= 6.0, m = 1g/L, t = 180min (live biomass), 90min (autoclaved biomass) and 30min (dried biomass).

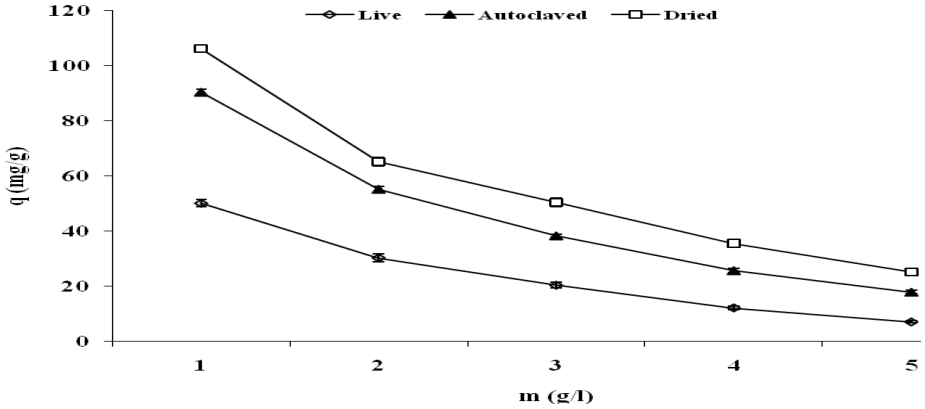

Fig. 6. Effect of biosorbent dose (m) on Cu(ll) uptake capacity of live, autoclaved and dried biomass of *Y. lipolytica* AUMC 9256. Biosorption conditions: Initial pH= 6.0; (Ci) =450 mg/L; t = 180min (live biomass), 90min (autoclaved biomass) and 30min (dried biomass).

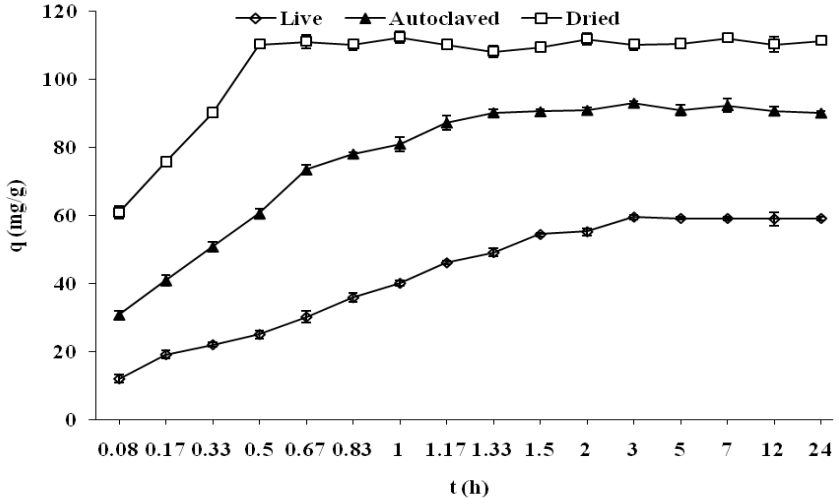

Fig. 7. Effect of contact time (t) on Cu(ll) uptake capacity of live, autoclaved and dried biomass of *Y. lipolytica* AUMC 9256. Biosorption conditions: Initial pH= 6.0; Ci = 450mg/L; m = 1g/L.

Characterization of Cu NPs synthesized by Y. lipolytica AUMC 9256

The UV-Visible spectra of CFS of biomass after Cu(II) uptake was recorded at λ_{max} 672, 368 nm (live), 368nm (autoclaved) and 670 and 368nm (dried) as shown in Fig. 8(a- c). The surface plasmon peak at 670 and 384nm indicated the formation of Cu NPs (Cuevas et al., 2015).

TEM images of Cu NPs (Fig. 9) showed that the mycosynthesized Cu NPs were spherical in shape with sizes 32.85 ± 9.67 nm (live), 22.34±4.5nm (autoclaved) and 15.62±4.0nm (dried).

Mechanism of Cu(II) removal

Transmission electron microscopy (TEM)

Ultra-thin sections of unloaded-live cells (control) revealed a distinct and smooth cell wall, plasma membrane, clear cytoplasm with normal nuclear membrane and few electron-dense areas probably representing the genetic material and cytoplasmic deposits (Fig. 10a). Cu(II)-loaded live cells exhibited dark electron opaque regions adsorbed tightly to the outer layers of the cell wall, within the cell wall layers and the cell interior indicating extracellular and intracellular sequestration of accumulated Cu(II). Plasmolysis with wide irregular periplasm containing many electron-dense granules and undulated plasma membrane were very obvious. Organelles couldn't be recognized (Fig. 10b). Needle-, rod-shaped precipitates were very clear within the central large vacuole (Fig. 10c). Some cells become extensively damaged with no cell wall, plasma membrane or cytoplasmic organelles (Fig. 10d). From TEM micrographs of Cu(II)-loaded autoclaved and dried cells (Fig. 10e, f and h, respectively), it can be found that extracellular precipitation of Cu(II) was the dominant mechanism in Cu(II) uptake.

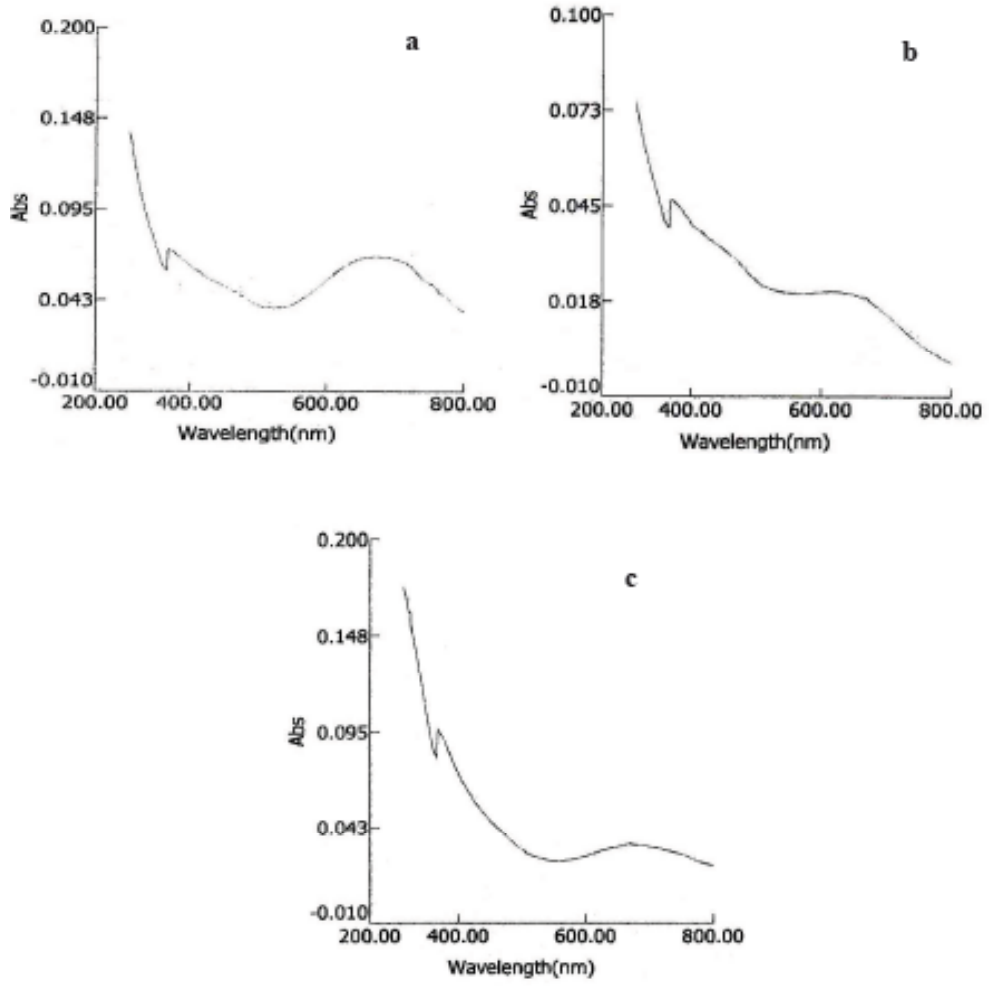

Fig. 8. UV-visible spectra of cell free supernatant (CFS) of *Y. lipolytica* AUMC 9256 (a) Live (b) Autoclaved, (c) Dried biomass after Cu(ll) uptake.

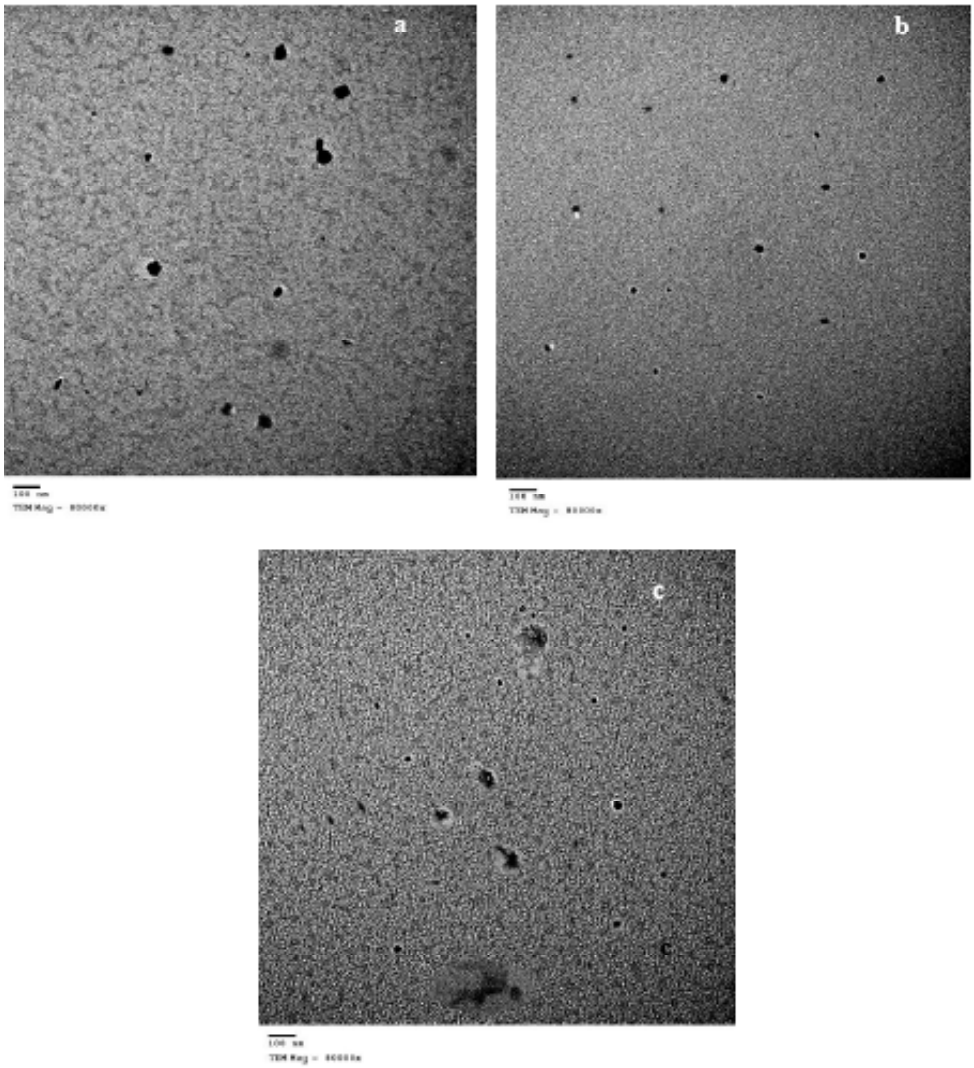

Fig. 9. TEM micrographs of Cu NPs synthesized by (a) Live biomass, (b) Autoclaved biomass, (c) dried biomass.

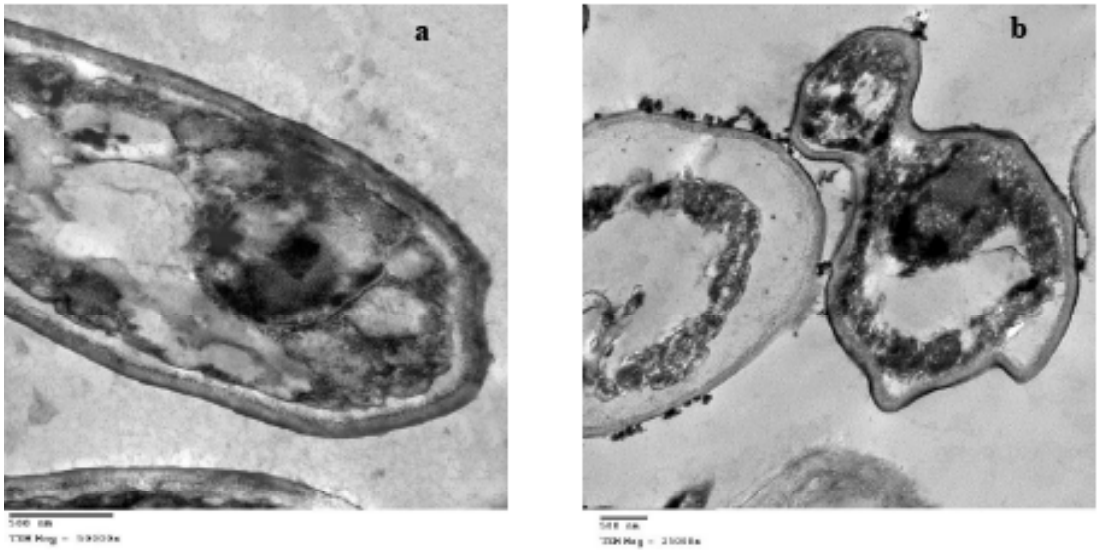

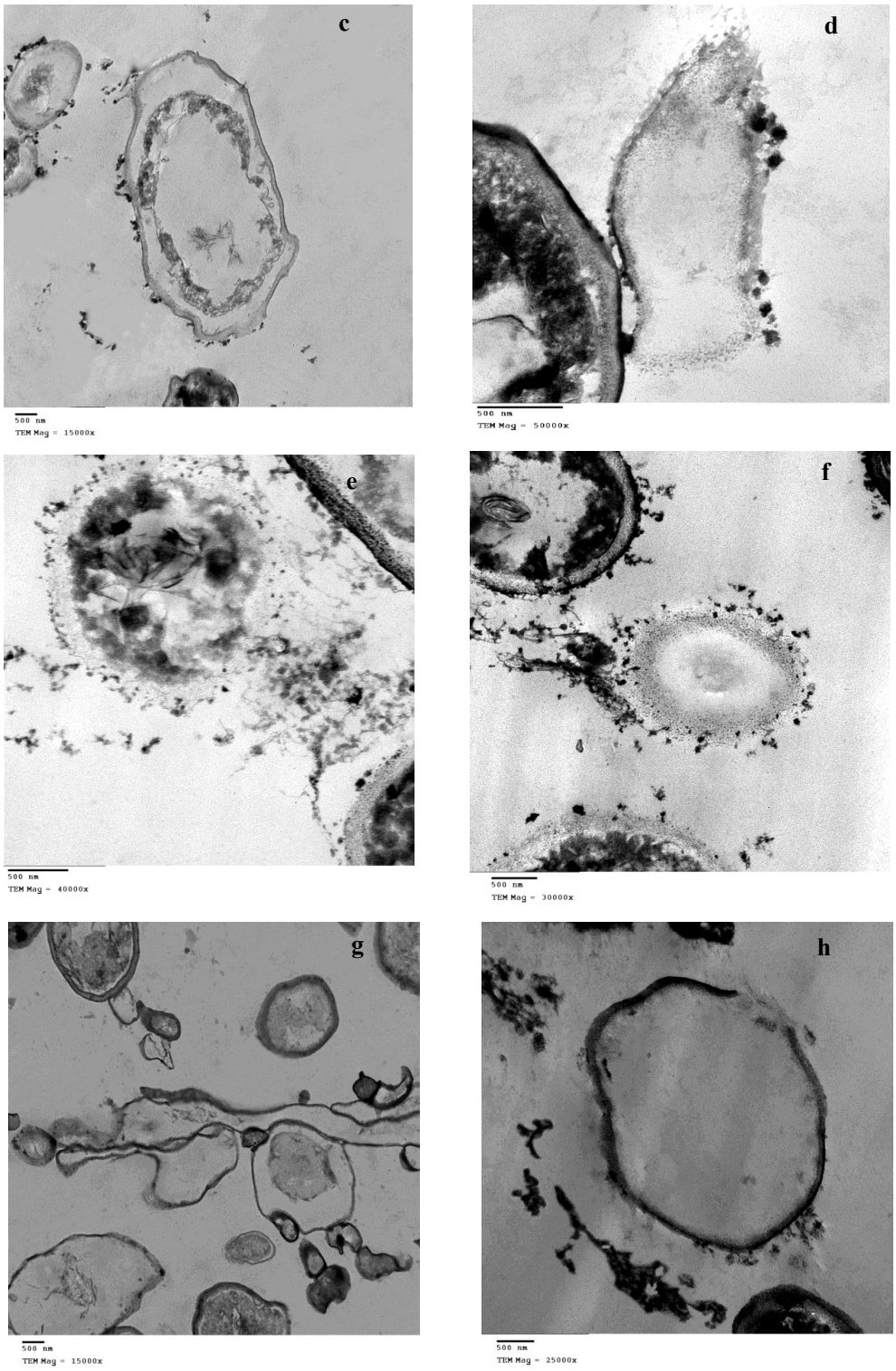

Fig. 10. TEM of *Y. lipolytica* AUMC 9256 (a) Native live biomass, (b-d) Cu(ll)-loaded live biomass, (e and f) Cu(ll)-loaded autoclaved biomass, (g) Native dried biomass, (h) Cu(ll)-loaded dried biomass.

FTIR spectroscopy

The FTIR spectra of metal-unloaded and metal-loaded biomass (live, autoclaved and dried) were shown in Fig. 11(a-d), respectively. There was a marked equal shifting at the wavenumber 3421 and 2925cm^{-1} in the case of live and autoclaved biomass (Fig. 11b and c, respectively) indicating the interaction of alcoholic -OH groups and amide -NH stretching vibration of primary amines and asymmetric stretching vibrations of C-H bonds from alkyl group in proteins and carbohydrates, respectively, with Cu(II) uptake. The appearance of new peaks at the wave number 2859cm^{-1} (live biomass) can be assigned to -CH stretching vibrations of CH_2- CH_3. The disappearance of the band at 2362cm^{-1} (live and autoclaved biomass) verifies the chemical interaction between Cu(II) and P-H phosphine and -NH stretching vibration of protonated amino (NH_2^+, NH^+). The disappearance of peaks at the wave number 2139cm^{-1} was indicative of alkynyl C=C, C ≡ C stretching vibrations and symmetric P-O-H stretching. The appearance of new shoulders at 1720cm^{-1} (autoclaved biomass) was due to C=O stretching of amides and carboxylic acids. Again a marked shifting at the wave number 1649cm^{-1} with a significant increase in the intensity can be attributed to alkene C= C stretching and C=O stretching mode conjugated to NH deformation mode and amide I band. The disappearance of shoulders at the wavenumber 1440 and 1366cm^{-1} was due to N=O stretching of amides and sulfonyl and sulfonamide groups and amide II, respectively. AbdelRahim et al. (2017) mentioned that changes in wavenumber 1426 and 1684cm^{-1} affirmed the presence of capping protein that covered the synthesized nanoparticles. The appearance of the new shoulder at 1388cm^{-1} (autoclaved biomass) can be assigned to the symmetric C-H deformation and -CH_3 of alkane in Cu(II) biosorption. A shift of bands at 1543cm^{-1} with a significant increase in the intensity verifies the chemical interaction between Cu(II) and amide II: N-H and C-N vibrations of the peptide bond in different protein conformations. An equal shift at band 1404cm^{-1} can be assigned to -OH bending in carboxylic acids and C-N stretching of amide II band. The absence of the band at 1254cm^{-1} was indicative of PO_2 in DNA, RNA and phospholipids and -SO_3 groups. The appearance of a shoulder at the wave number 1277cm^{-1} (live biomass) was due to C-O stretching of carboxylic acids. A shift at bands 1074cm^{-1} in living and dried loaded biomass can be attributed to ß(1→3) glucan (The major structural component of the yeast cell wall; 28.8% w/w), S=O and C-N stretching vibrations of amino groups. Either the absence of peaks at 887cm^{-1} (live and autoclaved biomass) or marked shift (Δ 21cm^{-1}) and appearance of new peaks at 802cm^{-1} (dried biomass) can be assigned to mannans, phosphorus and P=S stretching of phosphorus compounds. The very significant shift at the wave number 605cm^{-1} and appearance of the new intense peak at 595cm^{-1} (dried biomass) can be accountable for C-S stretching, M (metal)-O, O-M-O, ring deformation and phosphate functional groups. Electrostatic attraction to phosphate and carboxyl groups (of glucuronic acid) and amine groups of the chitosan and complexation with N or O donors (e.g. of chitin) may occur (Naja et al., 2005). The rate of C-S stretching of sulfur compounds can be observed again in the appearance of new intense peaks (autoclaved biomass) at 419 and 441cm^{-1}. It can be observed that OH bending of carboxylic acids, C-N stretching of amide II band are involved equally in Cu(II) uptake by three biomass. Mannans, phosphorus, P=S stretching, C-S stretching, M-O and ring deformation were more included in Cu(II) uptake by dried biomass.

Energy dispersive X-ray microanalysis (EDX)

The *EDX spectr*um of the metal-free biomass (Fig. 12a) exhibited distinct peaks of phosphorus, sulfur, potassium, and zinc, with element 34.83%, 18.70, 40.69 and 5.67, respectively, indicating the substantial presence of these elements. EDX analysis revealed that the high-intensity characteristic peaks of Cu(II) with element 47.5 % (live biomass, Fig. 12b), 55.29 (autoclaved biomass, Fig. 12c) and 59.72 (dried biomass, Fig. 12d) only exist after Cu(II) uptake. The atomic % of sulfur increased proportionally from 21.13% (control) to 50.95 (live biomass), 53.50% (autoclaved biomass) and 43.43 (dried biomass) with Cu(II) uptake. What is an important to underline is a sharp reduction of atomic % of phosphorus and potassium from 37.24, 35.21% (control) to 11.83, 4.96% (live biomass), 3.45, 0.86% (autoclaved biomass) and 12.26, 1.55% (dried biomass), respectively, following biosorption.

X-ray powder diffraction (XRD) analysis

The yeast strain biomass was subjected to XRD analysis before and after Cu(II) sorption (Fig. 13a-d). XRD spectrum for unloaded biomass confirmed its amorphous nature (Fig.13a). Cu(II)-loaded live biomass showed 6 peaks at 2θ: 16.66, 17.59, 18.76, 19.54, 20.63 and 28.80Å and corresponding to d-spacing 5.32, 5.04, 4.73, 4.54, 4.30 and 3.10Å. Based on spacing values these peaks are attributed

to the presence of the crystalline copper sulfite (Cu_2SO_3) and $Cu_3(SO_3)_2$ with average size particles 32.9 nm (Fig. 13b). Cu(II)-loaded autoclaved biomass showed 6 intense peaks at 2θ: 18.66 , 22.13 , 33.85, 25.05, 27.08 and 32.43Å and corresponding d-spacing value 4.75, 4.01, 3.73, 3.55, 3.29 and 2.76Å. Based on these spacing values, the peaks are attributed to the presence of crystalline copper sulfate ($Cu\ SO_4(H_2O)_5$) with average crystal size 28.83nm (Fig. 13c). The XRD pattern of dried biomass showed 4 peaks at 2θ: 18.60, 19.92, 20.86 and 32.22 Å and corresponding to respective d-spacing 4.77, 4.45, 4.73, 4.26 and 2.78 Å. Based on spacing values, these peaks are attributed to the presence of crystalline copper sulfate ($Cu\ SO_4(H_2O)_5$) (as in autoclaved biomass) (Fig. 13d).

Adsorptive removal of Cu(II) by dried Y. lipolytica AUMC 9256 biosorbent from environmental samples

pH value, temperature and Cu(II) concentration of ceramic wastewater were 8.33, 35°C and 21.2 mg/L, respectively. The extraction percentage of Cu(II) was identified in the range 42.7 (first run), 66.2 (second run) and 76.3 (third run).

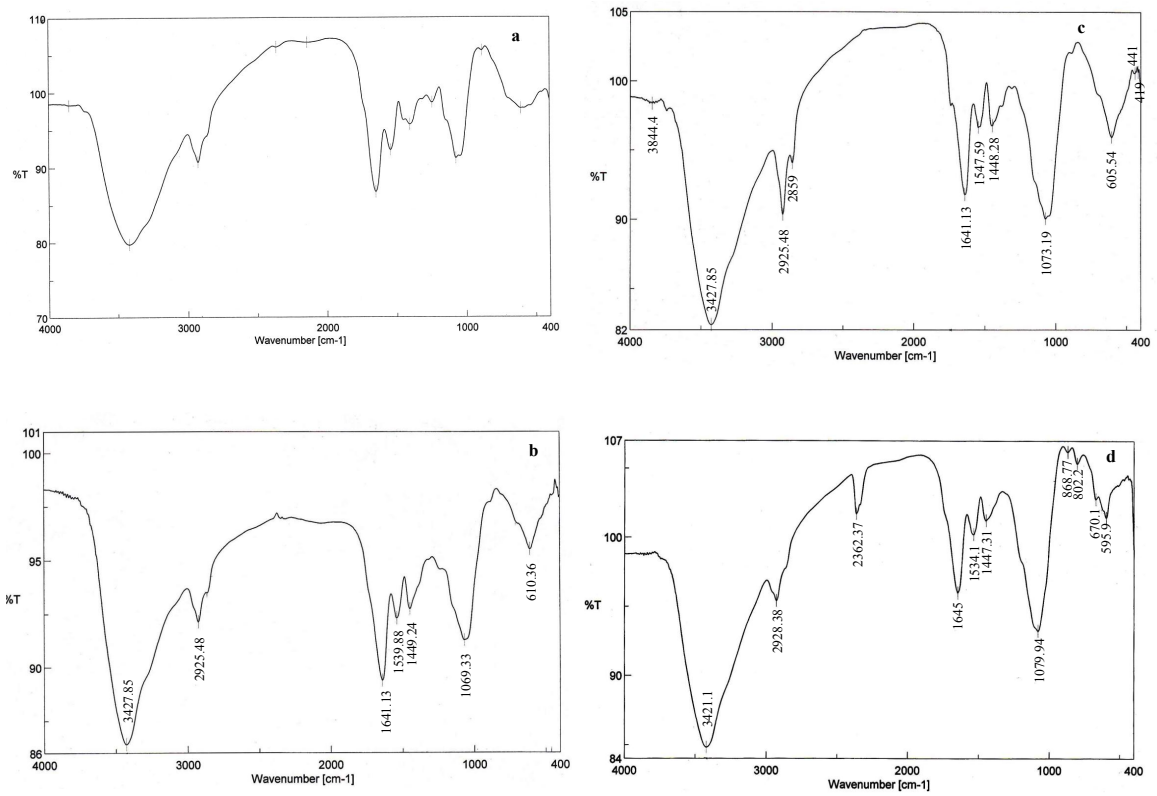

Fig. 11. FTIR spectra of *Y. lipolytica* AUMC 9256 (a) Native biomass, (b) Cu(ll)-loaded live biomass, (c) Cu(ll)-loaded autoclaved biomass, (d) Cu(ll)-loaded dried biomass.

Discussion

The test of the toxicity in solid media could be valuable in the evaluation of metal diffusion, and availability of metals are different from those observed in liquid media (Hassen et al., 2001). Metal tolerance studies are significant during bioremoval studies (Singh et al., 2013). The tolerance of *Y. lipolytica* AUMC 9256 to Cu(II) (1900mg Cu(II)/l) was higher than that was reported by Garcia et al. (2002) (480mg Cu(II)/L) and lesser than that was found by Bankar et al. (2012) (2010mg Cu(II)/L). Zinjarde et al. (2014) attributed the tolerance and detoxification of metals by *Y. lipolytica* to (i) Flushing out through efflux system, (ii) Production of metal binding biomolecules such as melanin and cysteine-rich metallothioneins, (iii) Enhanced production of superoxide dismutase (SOD) and H^+ATPase and (iv) Sequestration at the level of cell wall and plasma membrane. Dark color of colonies in the presence of Cu(II) is probably due to intensification of pigments on cell wall as a response to the stress applied by Cu(II). Similar results were reported by El-Sayed (2013) during the removal of lead(II) using *Saccharomyces cerevisiae*.

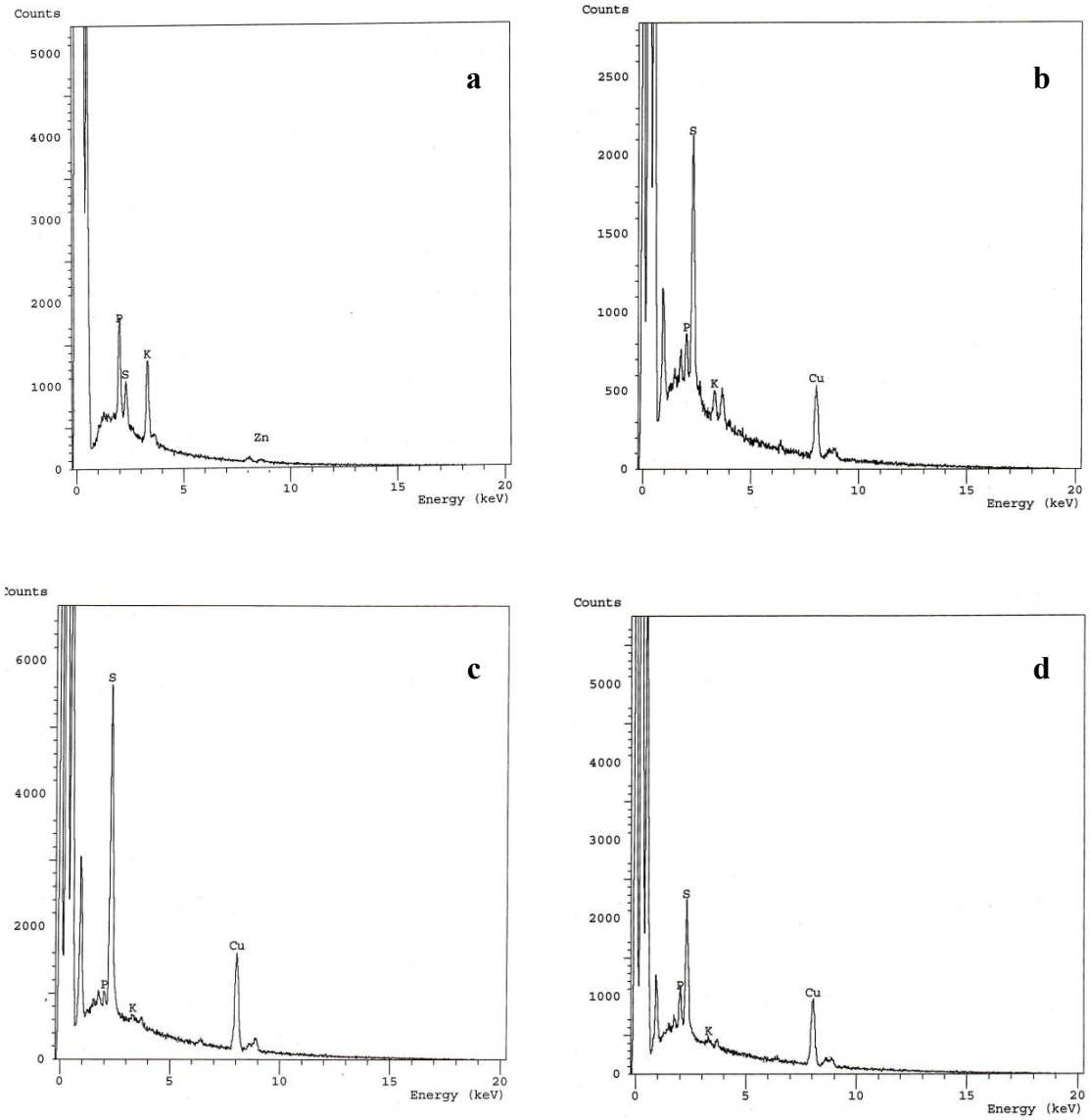

Fig. 12. EDX analysis of *Y. lipolytica* AUMC 9256 (a) Native biomass, (b) Cu(ll)-loaded live biomass (c), Cu(ll)-loaded autoclaved biomass, (d) Cu(ll)-loaded dried biomass.

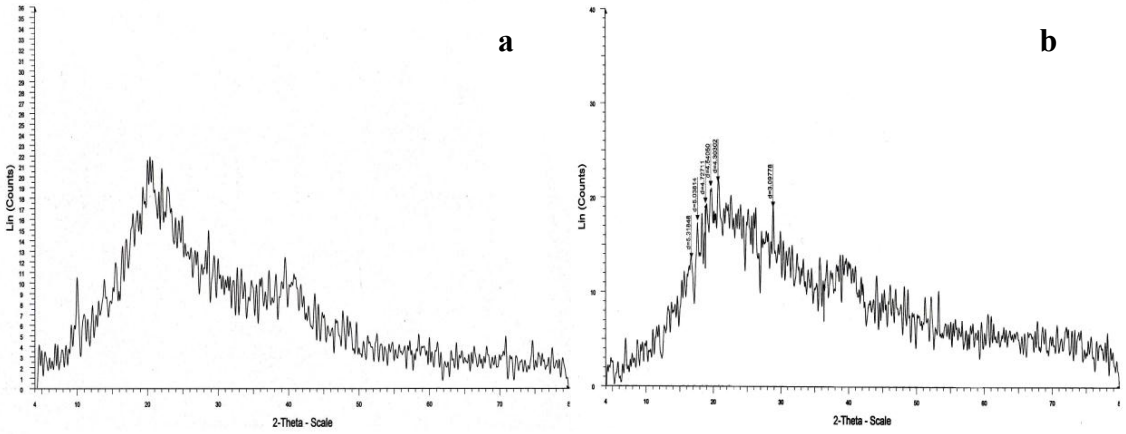

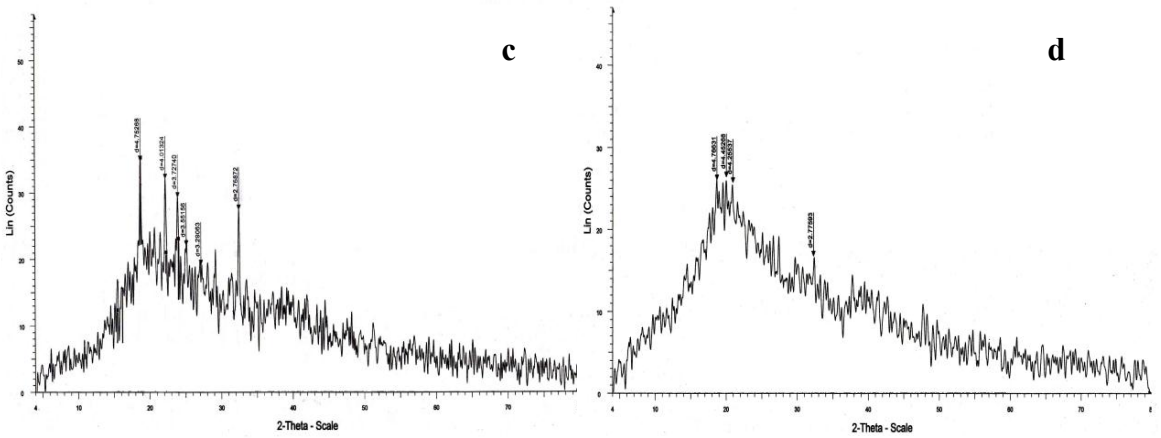

Fig. 13. XRD analysis of *Y. lipolytica* AUMC 9256 (a) Native biomass, (b) Cu(ll)- loaded live biomass, (c) Cu(ll)-loaded autoclaved biomass, (d) Cu(ll)-loaded dried biomass.

To avoid the protective chelating effect of agar, it was very important to cultivate *Y. lipolytica* strain in a broth culture medium containing different concentrations of Cu(II). Although the yeast strain was able to tolerate high concentration of Cu(II) (1900mg/L) on solid media, in liquid media the tolerance was lesser (800mg/L). In this respect, Adamo et al. (2012) observed that on minimal broth medium, 0.5g/L $CuSO_4$ was sufficient to inhibit the growth of all tested yeast strains, whereas on rich YPD plates all of them tolerated up to 1g/L $CuSO_4$. They concluded that the composition of the culture medium and the growth conditions affect Cu(II) sensitivity of yeast cells. A primary increase in the growth of *Y. lipolytica* in the presence of 100mg Cu(II)/L may be due to the fact that the low dose of Cu(II) triggered Arndt-Schultz effect, regarding to which toxic metals in non-lethal doses may induce instability in the cell membrane permeability that may cause more free flow of nutrients within the cell and hence the metabolic activities induced (Ahonen-Jonnarth et al., 2004). On contrary, at high concentrations (750mg Cu(II)/L), the redox-active heavy metals such as Cu(II) and Co(II) enable redox reactions in the cell, for example, $Cu(II) \leftrightarrow Cu(I) + e^-$ (Valko et al., 2005). They are involved in the formation of $OH^\bullet$ from H_2O_2 via Haber-Weiss and Fenton reactions and initiate non-specific lipid peroxidation and oxidize biomolecules of the cell (Sharma & Dietz, 2009).

An increase in Cu(II) concentration resulted in a decrease in biomass production and positively correlated with increased residual Cu(II) in the culture broth and led to a decline in R_e%. Also, metal ions in the solution would not only be adsorbed to the surface of the biomass, but also enter the intracellular part through facilitating the concentration gradient of metal ions. Metal ions can also enter into the cell if the cell wall was disrupted. The results of this study are in the line with the observations of Nongmaithem et al. (2016) and Perez-Rama et al. (2002). The release of Ca(II) and K(I) indicated that ion exchange may be the dominant mechanism in biosorption (Naja & Velosky, 2011).

pH is a critical factor in biosorption of metal ions that influences electrostatic binding of ions to corresponding functional groups (El-Gendy et al., 2017). At acidic pH 2, the sorption sites, whatever the type of the biomass, are surrounded by hydronium ions (H_3O^+) and negative charge intensity was reduced. This suggests that the mechanism is related to covalent bonds and not to an electrostatic interaction in this pH value (Labuto et al., 2015). As the pH increases, relatively more amounts of OH ions within the solution will present and more ligands, such as carboxyl, hydroxyl, amino and phosphoryl groups that carry more negative charges were exposed and may bind cationic metals (Mihaiescu et al., 2016). The Cu(II) biosorption capacity of dried cells was higher than that of autoclaved and live ones. It seemed that heat treatment caused an increase in the accessibility of the metal ions to the metal-binding sites on the biomass (Ghorbani et al., 2008). At a low initial solute (50mg Cu(II)/L), the ratio of the biosorbent surface to the metal ions was higher and therefore most of them reacted with the biosorbent and were

removed (Bankar et al., 2012). An increase in the loading capacities of the biomass with increasing metal ion concentrations is probably due to that the initial metal ion concentrations may provide a driving force that increases adsorption process and more of metal ions may compete for the limited sites of the biomass surface (Nguema et al., 2014). A decrease in the biosorption capacity with an increase in biomass dosage can be explained by "mass effect", meaning that aggregation of abundant biosorbents will cause an increment in the electrostatic interaction, an interference among binding sites and reduce the surface area available to Cu(II) ions (Nguema et al., 2014). Additionally, at the high biosorbent dosage, the available solute was insufficient to completely cover the available exchangeable sites on the biosorbent, thus causing low solute uptake (Tangaromsuk et al., 2002).

One of the strategies used by *Y.lipolytica* to tolerate the heavy metal toxicity is nanoparticle synthesis (Zinjarde et al., 2014). The appearance of green-blue color after the addition of $CuSO_4$ to the colorless CFS suggested the reduction of Cu(II) and the formation of Cu NPs. Some organic functional groups of microbial cell walls were involved in the reduction of metal ions by dead biomass (Lin et al., 2001).

In order to give a better understanding on the adsorption mechanism of *Y. lipolytica* AUMC 9256 to Cu(II), TEM, FTIR, EDX and XRD were used to observe the ultrastructure changes, functional groups that were involved in bioremoval process, elemental transformation and crystalinity. Ultrathin sections of Cu(II)-loaded live cells exhibited dark electron opaque regions adsorbed tightly to the outer layers of the cell wall, within the cell wall layers and the cell interior indicating extracellular and intracellular sequestration of accumulated Cu(II). This may take place based on a variety of chemical binding means (chemisorption). Examples of chemisorption are metal complexation and chelation onto cell wall which seemed to be the first defense of *Y. lipolytica* against toxicity of high concentration of Cu(II) (avoidance mechanism) (Naja & Velosky, 2011). Many electron-dense granules were localized within the periplasm where melanin was present to prevent Cu(II) from entering the cytosol (Ito et al., 2007). The reason of cytoplasm shrank might be related with the lipid over oxidation of cell plasma membrane (Sun et al., 2015). Needle-, rod-shaped precipitates were very clear within the central large vacuole. Van der Heggen et al. (2010) reported that Pb (II) is conjugated with glutathione in the cytoplasm of *S. cerevisiae* and the lead glutathione complex is transported to the vacuole. FTIR spectra cleared that dried biomass incurred the highest changes (Δ 149cm^{-1}) during Cu(II) uptake. Degraded cells would offer a larger available surface area and expose the intercellular constituents and more surface binding sites due to the destruction of the cell membranes (Errasquim & Vazquez, 2003). The results of this study disagreed with Labuto et al. (2015) who stated that heating (wet or dry) can cause a loss of secondary or tertiary structure of cell wall proteins and changes in functional groups' availability and exposure. EDX analysis revealed a sharp reduction of atomic % of phosphorus and potassium following Cu(II) uptake. The reduction of intracellular potassium, further illustrated that ion exchange was involved in the biosorption of Cu(II) to maintain ionic balance across the membrane (Isaac & Sivakumar, 2013). The reduction of cellular polyphosphate content of *Y. lipolytica* might be due to the involvement of cellular polyphosphate in the formation of Cu(II)-phosphate complexes. These complexes are located near the cell surface and hence might be excluded from the medium with the help of some amino acids (Ito et al., 2007). An increase in atomic % of sulfur may be due to the formation of precipitates in the form of sulfate on the cell surface (Xia et al., 2015). From EDX analysis, it can be concluded that ion exchange, intracellular and extracellular precipitation may be included in Cu(II) uptake by *Y. lipolytica* AUMC 9256. XRD is a unique non- destructive method used to distinguish between amorphous and crystalline materials and to quantify the perfect crystallinity of the sample. XRD spectra for Cu(II)-loaded biomass confirmed its crystalline nature The crystalline formation following a long period of metal accumulation could be due to the complexation of metal ions and metal precipitation in a crystalline state (Lopez et al. 2000).

The passive biosorption uptake of metals by dried biomass appears as a powerful tool for somewhat selectively removing heavy metals ions from solution. Immobilization of dissolved toxic heavy metals and their physical removal by biosorption in a water purification process is not only technically convenient but it may prove to be economically quite attractive (Naja & Velosky, 2011). According to the extraction percentage

of Cu(II) which ranged from 42.7 to 76.3, the results of this study provide good evidence for the potential applications of dried *Y. lipolytica* AUMC 9256 biosorbent for removal of Cu(II) ions from real water samples.

Conclusion

The *Yarrowia lipolytica* AUMC 9256 showed the ability to synthesize copper nanoparticles during the bioremediation of copper by living, autoclaved and dried biomass. Copper nanoparticles were all spherical in shape with different particle size depending on the type of biomass. The occurrence of extracellular complexation, precipitation, adsorption onto cell wall, and sequestration of needle-, rod-shaped precipitates within central large vacuole during were the dominant mechanisms during Cu(II) uptake. EDX analysis further illustrated that ion exchange was very important in the biosorption of Cu(II). FTIR spectra cleared that dried biomass incurred the highest changes (Δ 149 cm^{-1}) during Cu(II) uptake. The results claimed that the dried biomass *Y. lipolytica* AUMC 9256 can be used with high efficiency as s biosorbent for removal of Cu(II) ions from real water samples.

References

AbdelRahim, K., Mahmoud, S.Y., Ali, A.M., Almaary, K.S., Mustafa, A.M.A. and Husseiny, S.M. **(**2017) Extracellular biosynthesis of silver nanoparticles using *Rhizopus stolonifer*. *Saudi J. Biol. Sci.* **24**, 208-216.

Adamo, G.M., Brocca, S., Passolunghi, S., Salvato, B. and Lotti, M. (2012) Laboratory evolution of copper tolerant yeast strains. *Microb. Cell Fact*. **11**, 1-11.

Adams, G.O., Fufeyin, P.T., Okoro, S.E. and Ehinomen, I. (2015) Bioremediation, biostimulation and bioaugmentation: A Review. *Int. J. Environmental Bioremediation & Biodegradation,* **3**(1), 28-39.

Ahonen-Jonnarth, U., Roitlo, M., Markkola, A.M., Ranta, H. and Neuvonen, S. (2004) Effects of nickel and copper on growth and mycorrhiza of Scots pine seedlings inoculated with Gremmeniellabietina. *For. Pathol.* **34,** 337-348.

Akinkunmi, W., Husaini, A., Zulkharnain, A., Guan, T. and Roslan, H. (2016) Mechanism of biosorption of Pb(II) and Cu(II) ions using dead biomass of *Fusarium equiseti* strain UMAS and *Penicillium citrinum* strain UMAS B2. *J. Biochem. Microbiol. Biotechnol. (JOBIM*) **4**(2), 1-6.

Ali, H., Khan, E. and Sajad, M.A. (2013) Phytoremediation of heavy metals-concepts and applications. *Chemosphere,* **91**, 869-881.

Anju, M. (2017) Biotechnological strategies for remediation of toxic metal(loids) from environments. In: "*Plant Biotechnology: Recent Advancements and Developments*", Springer Science+Business Media B.V.

Bankar, A.V., Zinjarde, S.S. and Kapadnis, B.P. (2012) Management of heavy metal pollution by using yeast biomass. In: "*Microorganisms in Environmental Management: Microbes and Environment*", © Springer Science + Business Media B.V.

Buss, W., Kammann, C. and Koyro, H.W. (2012) Biochar reduces copper toxicity in *Chenopodium quinoa* willd. in a sandy soil. *J. Environ. Qual*. **41,** 1157-1165.

Coelho, M.A.Z., Amaral, P.F.F. and Belo, I. (2010) *Yarrowia lipolytica*: An industrial workhorse. In: "*Current ResearchTechnology, Education Topics in Appl. Microbiol. and Microb. Biotechnol.*", A. Mendez-Vilas (Ed.), pp.930-944. Formatex Research Center, Spain.

Cuevas, R., Durán, N., Diez, M.C., Tortella, G.R. and Rubilar, O. (2015) Extracellular biosynthesis of copper and copper oxide nanoparticles by *Stereum hirsutum*, a native white-rot fungus from Chilean Forests. *J. Nanomater.* **2015**, 1-7, Article ID 789089.

Dhankhar, R. and Hooda, A. (2011) Fungal biosorption-an alternative to meet the challenges of heavy metal pollution in aqueous solutions. *Environ. Technol*. **32**, 467-491.

El-Gendy, M.M., Hassanein, N.M., Ibrahim, H.A. and Abd El-Baky, D.H. (2017) Heavy metals biosorption from aqueous solution by endophytic *Drechslera hawaiiensis* of *Morus alba* L. derived from heavy metals habitats. *Mycobiology,* **45**(2), 73-83.

El-Sayed, M.T. (2013) Removal of lead(II) by *Saccharomyces cerevisiae* AUMC 3875. *Ann. Microbiol*. **63,** 1459-1470.

Errasquim, E.L. and Vazquez, C. (2003) Tolerance and uptake of heavy metals by *Trichoderma atroviride*

isolated from sludge. *Chemosphere,* **50**(1), 137-143.

Garcia, S., Prado, M., Dégano, R. and Domínguez, A. (2002) A copper responsive transcription factor, CRF1, mediates copper and cadmium resistance in *Yarrowia lipolytica*. *J. Biol. Chem*. **277**(40), 37359-37368.

Ghorbani, F., Younesi, H., Ghasempouri, S.M., Zinatizadeh, A.A., Amini, M. and Daneshi, A. (2008) Application of response surface methodology for optimization of cadmium biosorption in an aqueous solution by *Saccharomyces cerevisiae*. *Chem. Eng. J*. **145**(2), 267-275.

Hassen, A., Saidi, N., Cherif, M. and Boudabous, A. (2001) Resistance of environmental bacteria to heavy metals. *Bioresour. Technol*. **64**, 7-15.

Huang, F., Dang, Z., Guo, C., Lu, G., Xu, R.R., Liu, H. and Zhang, H. (2013) Biosorption of Cd(II) by live and autoclaved cells of Bacillus cereus RC-1 isolated from cadmium. contaminated soil. *Colloids Surf*. B **107**, 11-18.

Isaac, C.P. and Sivakumar, A. (2013) Removal of lead and cadmium ions from water using *Annona squamosa* shell: Kinetic and equilibrium studies. *Desalination and Water Treatment,* **51**, 7700-7009.

Ito, H., Inouhe, M., Tohoyama, H. and John, M. (2007) Copper extrusion after accumulation during growth of copper-tolerant yeast *Yarrowia lipolytica*. *Z. Naturforsch*. **62**, 77-82.

Karbassi, A.R., Tajziehchi, S. and Farhang, A.N. (2016) Role of estuarine natural processes in removal of trace metals under emergency situations. *Global J. Environ. Sci. Manag*. **2**, 31-38.

Labuto, G., Trama, B., Da Vitorino Silva, F., Collazo, R., Da Silveria Gueller, G.C. and de Souza Guarnieri, B. (2015) Metals uptake by live yeast and heat-modified yeast residue. *Revista Ambiente Àgua,* **10**(3), 510-519.

Lin, Z.Y., Fu, J.K., Wu, J.M., Liu, Y. and Cheng, H, (2001) Preliminary study on the mechanism of non-enzymatic bioreduction of precious metal ions. *Acta Phys-Chim Sin*. **17**, 477-480.

Lopez, A., Lazaro, N., Priego, J.M. and Marques, A.M. (2000) Effect of pH on the biosorption of nickel and other heavy metals by *Pseudomonas fluorescens* 4F39. *J. Ind. Microbiol. Biotechnol*. **24**(1), 146-151.

Mahmoud, M., Zokm, G., Farag, A. and Abdelwahab, M. (2017) Assessment of heat-inactivated marine *Aspergillus flavus* as a novel biosorbent for removal of Cd(II), Hg(II) and Pb(II) from the water. *Environ. Sci. Pollut. Res*. **24**, 18218-18228.

Mihaiescu, T, Stanila, A., Odagiu, A. and Mihăiescu, R. (2016) Assessment of copper and lead biosorption from aqueous solutions by brewer's yeast. *Pro. Environment.* **9**, 430-434.

Naja, G., Mustin, C., Volesky, B. and Berthelin, J. (2005) A high-resolution titrator: A new approach to studying binding sites of microbial biosorbents. *Water Res*. **39**, 579-588.

Naja, G. and Volesky, B. (2011) The mechanism of metal cation and anion biosorption, In: "*Microbial Biosorption of Metals*", P. Kotrba, M. Mackova, T. Macek (Ed.). © Springer Science + Business Media B.V.

Nguema, P.F., Luo, Z. and Lian, J. (2014) The biosorption of Cr(VI) ions by dried biomass obtained from a chromium-resistant bacterium. *J. Front. Chem. Sci. Eng*. **8**(4), 454-464.

Nongmaithem, N., Roy, A. and Bhattacharya, P.M. (2016) Screening of Trichoderma isolates for their potential of biosorption of nickel and cadmium. *Braz. J. Microbiol*. **47**, 305-313.

Oyetibo, G.O., Miyauchi, K., Suzuki, H. and Endo, G. (2016) Mercury removal during growth of mercury tolerant and self-aggregating *Yarrowia* spp. *AMB Expr*. **6**, 99-110.

Paš, M., Milačič, R., Drašar, K., Pollak, N. and Raspor, P. (2004) Uptake of chromium(III) and chromium(VI) compounds in the yeast cell structure. *Biometals* **17**, 25-33.

Perez-Rama, M., Alonosa, J.A., Lopez, C.H. and Vaamonde, E.T. (2002) Cadmium removal by the living cells of the marine microalgae *Tetraselmis suecica*. *Bioresource Technol.* **84**, 265-270.

Sağ, Y., Nourbakhsh, M., Aksu, Z. and Kutsal, T. (1995)Comparison of Ca-alginate and immobilized *Z. ramigera* as sorbents for copper(II) removal. *Process Biochem.***30**, 175-181.

Shanab, S., Essa, A. and Shalaby, E. (2012) Bioremoval capacity of three heavy metals by some microalgae species (Egyptian isolates). *Plant Signal. & Behav.* **7**(3), 392-399.

Sharma, S.S. and Dietz, K.J. (2009) The relationship between metal toxicity and cellular redox imbalance. *Trends Plant Sci*. **14**(1), 43-50.

Siddiqi, K.S. and Husen, A. (2016) Fabrication of metal nanoparticles from fungi and metal salts: Scope and application. *Nanoscale Res. Lett.* **11**(98), 1-15.

Singh, P., Raghukumar, C., Parvatkar, R.R. and Mascarenhas-Pereira, M.B.L. (2013) Heavy metal tolerance in the psychrotolerant *Cryptococcus* sp. isolated from deep-sea sediments of the Central Indian Basin. *Yeast,* **30**, 93-101.

Sun, X.Y., Zhao, Y., Liu, L., Jia, B., Zhao, F., Huang, W., et al. (2015) Copper tolerance and biosorption of *Saccharomyces cerevisiae* during alcoholic fermentation. *PLoS ONE,* **10**(6), e0128611. doi:10.1371/journal.pone.0128611

Tangaromsuk, J., Pokethitiyook, P., Krutarachue, M. and Upatham, E.S. (2002) Cadmium biosorption by *Sphingomonas paucimobilis* biomass. *Bioresour. Technol*. **85**(1), 103-105.

Valko, M., Morris, H. and Cronin, M.T. (2005) Metals, toxicity and oxidative stress. *Curr. Med. Chem*. **12**(10), 1161-1208.

Van der Heggen, M., Martins, S., Flores, G. and Soares, E.V. (2010) Lead toxicity in *Saccharomyces cerevisiae*. *Appl. Microbiol. Biotechnol*. **88,** 1355-1361.

Vijayaraghavan, K. and Balasubramanian, R. (2015) Is biosorption suitable for decontamination of metal-bearing wastewaters? A critical review of the state-of-the-art of biosorption processes and future directions. *J. Environ. Manag*. **160**, 283-296.

WHO (2004) Copper in Drinking Water. A major public health concern 20 Avenue Appia, 1211 Geneva 27, Switzerland.

Wierzba, S. (2017) Biosorption of nickel(II) and zinc(II) from aqueous solutions by the biomass of yeast Yarrowia lipolytica. *Polish J. Chem. Technol.* **19**(1), 1-10.

Xia, L., Xu, X., Zhu, W., Huang, Q. and Chen, W. (2015) A comparative study on the biosorption of Cd^{2+} onto *Paecilomyces lilacinus* XLA and *Mucoromycote* sp. XLC. *Int. J. Mol. Sci*. **16,** 15670-15687.

Zinjarde, S., Apte, M., Mohite, P. and Kumar, A.R. (2014) *Yarrowia lipolytica* and pollutants: Interactions and applications. *Biotechnol. Adv*. **32**(5), 920-933.

(*Received* 27/2/2018;
accepted 25/7/2018)

المعالجة البيولوجية لمياه الصرف الصحي والتصنيع خارج الخلية من الجسيمات النحاس النانوية من قبل ياروبا ليبوليتيكا

منال توفيق السيد
قسم النبات – كلية العلوم – جامعة الزقازيق –الزقازيق – مصر.

هذه أول دراسة تصف التكوين السريع خارج الخلية لجسيمات النحاس النانوية خلال المعالجة البيولوجية للنحاس بواسطة الكتلة الحيوية الحية والمعقمة والجافة من ياروبا ليبوليتيكا. تم دراسةالنمو في وجود تركيزات مختلفة من عنصرالنحاس. كان الحد الأدنى من تركيز المثبطة 1900 ملغم نحاس/ لتر. وتم تقييم التوزيع الخلوي لأيونات النحاس المتراكم أحيائيا. وقد تم تحقيق أقصى قدرات الأمتصاص في الرقم الهيدروجيني 6.0، وتركيزأولي لعنصر النحاس 450 ملغ/لتر، جرعة الكتلة الحيوية 1 غرام/لتر ووقت الاتصال 180 دقيقة للخلايا الحية، 90 دقيقة للمعقمة و 30 دقيقة للكتلة الحيوية الجافة. وتم تمييز الجسيمات النانوية النحاسية بالأشعة فوق البنفسجية الطيفي المرئي والمجهر الإلكتروني النافذ. وكشف الفحص بالمجهر الإلكتروني النافذ عن حدوث تعقيدات خارج الخلية، والامتصاص على جدار الخلية، واحتجاز الرواسب على شكل عصوي أو ابري داخل فجوة كبيرة مركزية خلال امتصاص عنصرالنحاس بواسطة الكتلة الحيوية الحية. وأكد التحليل الطيفي للأشعة تحت الحمراء أن مانانز والفوسفور، P = S، C - S، M - O و غيرها من المجاميع الفعالة ساهمت في امتصاص النحاس بواسطة الكتلة الحيوية الجافة. أكد التحليل الدقيق للأشعة السينية (إدكس) وجود نسب مميزة عالية الكثافة من النحاس. تم إزالة النحاس من مياه الصرف في صناعة السيراميك بواسطة الكتلة الحيوية المجففة بشكل فعال.